

Dynamical Masses for Low-Mass Pre-Main Sequence Stars: A Preliminary Physical Orbit for HD 98800 B

astro-ph version July 2, 2018

Andrew F. Boden^{1,2}, Anneila I. Sargent³, Rachel L. Akeson¹, John M. Carpenter³,
Guillermo Torres⁴, David W. Latham⁴, David R. Soderblom⁵, Ed Nelan⁵, Otto G. Franz⁶,
Lawrence H. Wasserman⁶

bode@ipac.caltech.edu

ABSTRACT

We report on Keck Interferometer observations of the double-lined binary (B) component of the quadruple pre-main sequence (PMS) system HD 98800. With these interferometric observations combined with astrometric measurements made by the Hubble Space Telescope Fine Guidance Sensors (FGS), and published radial velocity observations we have estimated preliminary visual and physical orbits of the HD 98800 B subsystem. Our orbit model calls for an inclination of 66.8 ± 3.2 deg, and allows us to infer the masses and luminosities of the individual components. In particular we find component masses of 0.699 ± 0.064 and $0.582 \pm 0.051 M_{\odot}$ for the Ba (primary) and Bb (secondary) components respectively.

Spectral energy distribution (SED) modeling of the B subsystem suggests that the B circumstellar material is a source of extinction along the line of sight to the B components. This seems to corroborate a conjecture by Tokovinin that the B subsystem is viewed through circumbinary material, but it raises important questions about the morphology of that circumbinary material.

¹Michelson Science Center, California Institute of Technology, 770 South Wilson Ave., Pasadena CA 91125

²Department of Physics and Astronomy, Georgia State University, 29 Peachtree Center Ave., Science Annex, Suite 400, Atlanta GA 30303

³Division of Physics, Math, and Astronomy, California Institute of Technology, MS 105-24, Pasadena, CA 91125

⁴Harvard-Smithsonian Center for Astrophysics, 60 Garden St., Cambridge MA 02138

⁵Space Telescope Science Institute, 3700 San Martin Dr, Baltimore, MD 21218

⁶Lowell Observatory, 1400 W. Mars Hille Road, Flagstaff, AZ 86001

Our modeling of the subsystem component SEDs finds temperatures and luminosities in agreement with previous studies, and coupled with the component mass estimates allows for comparison with PMS models in the low-mass regime with few empirical constraints. Solar abundance models seem to under-predict the inferred component temperatures and luminosities, while assuming slightly sub-solar abundances bring the models and observations into better agreement. The present preliminary orbit does not yet place significant constraints on existing pre-main sequence stellar models, but prospects for additional observations improving the orbit model and component parameters are very good.

Subject headings: binaries: spectroscopic — stars: fundamental parameters — stars: pre-main sequence — stars: individual (HD 98800)

1. Introduction

Accurate determinations of the physical properties of stars (e.g. mass, radius, temperature, luminosity, elemental abundance, etc.) provide fundamental tests of stellar structure and evolution models. The most basic of stellar physical properties is the mass, available only from the study of dynamical interactions – most typically in binary stars.

Among the areas where our understanding of stellar structure is most uncertain is in pre-main sequence (PMS) stars, particularly for low-mass systems (see Palla & Stahler 2001; Hillenbrand & White 2004, and references for summaries). Providing empirical constraints on models of PMS stars is critical for improving their accuracy, and the reliability of these models in turn is critical to our understanding of individual PMS systems in particular, and the process of star formation in general. So experimental determinations of masses and luminosities for PMS stars are of fundamental importance in constraining our understanding of star formation and early stellar evolution.

Eclipsing binary systems are important because of the favorable geometry for accurate mass and radius determination (e.g. Andersen 1991). However, component mass determinations for non-eclipsing spectroscopic binaries are possible with measurement of the orbital inclination. In order to expand the number of low-mass PMS systems with dynamical mass measurements, we have embarked on a program to estimate physical orbits in PMS systems by integrating interferometric and spectroscopic observations. This follows the initial determination of a non-eclipsing PMS system orbit for the T Tauri binary HBC 427 by Steffen et al (2001). Additionally Simon et al (2000) have used star-disk interactions to measure the mass of PMS stars. Hillenbrand & White (2004) provide a current summary of dynamical

mass determinations for pre-main sequence stars.

HD 98800 (HIP 55505, TWA 4A) is a well-studied quadruple star system in the TW Hya association. The system was first detected as a visual binary by Innes (1909); at current epoch the separation is roughly $0.8''$ on approximately a N-S line (Prato et al 2001, herein P2001). Torres et al. (1995, herein T95) established that both visual components are themselves spectroscopic binaries, finding a 262-day single-lined orbit for the primary (Southern, A) component, and a 315-day double-lined orbit for the secondary (Northern, B) component. The system exhibits a strong mid-infrared (IR) excess longward of $7 \mu\text{m}$ (Walker & Walstencroft 1988; Zuckerman & Becklin 1993), lithium signatures, but no signs of active accretion (Soderblom et al 1996; Webb et al 1999). The mid-IR excess, Li, HD 98800’s putative membership in the TW Hya association, and the Hipparcos distance estimate of 46.7 ± 6.2 pc (establishing component luminosities) lead to the consensus that the system is PMS. Soderblom et al (1998, herein S98) has termed the system “post-T Tauri”, and estimates a system age range of 5 – 20 Myr with a most likely value of 10 Myr based primarily on Li abundance. Multi-band IR imaging studies firmly establish that the mid-IR excess is associated with the double-lined B subsystem, most likely in the form of a circumbinary disk (see Koerner 2000, P2001, and references therein).

Here we report on observations of the double-lined HD 98800 B binary subsystem made with the Keck Interferometer (KI, Colavita et al 2003) and the Hubble Space Telescope Fine Guidance Sensor (FGS). These observations resolve the B subsystem and allow us to estimate the visual and physical orbits (in combination with radial velocity measurement from T95), and determine the component dynamical masses and luminosities. KI and FGS observations of HD 98800 B and our orbital solution are described in § 2. Physical parameters implied by the orbit and spectral energy distribution modeling are discussed in § 3. Finally a discussion of these results including comparisons with pre-main sequence stellar models is given in § 4.

2. Observations and Orbital Solution

KI Observations The KI interferometric observable used for these measurements is the fringe contrast or *visibility* (squared) of an observed brightness distribution on the sky. KI was used to make the interferometric measurements presented here; KI is a long-baseline *H* ($1.6\mu\text{m}$) and *K*-band ($2.2\mu\text{m}$) interferometer located at Mauna Kea, HI, and described in detail elsewhere (Colavita et al 2003). The analysis of such data on a binary system is discussed in detail in previous work (e.g. Boden et al. 2000; Hummel et al. 2001).

HD 98800 B was observed in conjunction with calibration objects by KI in *K*-band

($\lambda \sim 2.2\mu\text{m}$) on five nights between 18 April 2003 and 22 April 2005, a dataset spanning roughly two years and 2.3 orbital periods. HD 98800 B and relevant calibration objects were observed multiple times during each of these nights, and each observation (scan) was approximately 130 sec long. For each scan we computed a mean V^2 value from the scan data, and the error in the V^2 estimate is inferred from the rms internal scatter. HD 98800 B was always observed in combination with one or more calibration sources within $\sim 5^\circ$ on the sky. For this analysis we have used HD 97590 (A6 V) and HD 100219 (F7 V) as calibration objects; Table 1 lists the relevant observational parameters for the calibration objects. Calibrating our interferometric data with respect to these objects results in 34 calibrated visibility scans on HD 98800 B; these measurements are summarized in Table 2. Finally we will note that as the Keck Telescopes separately resolve the HD 98800 A-B system (P2001), and the KI beam combiner is fed by single-mode fiber, no light from HD 98800 A falls on the fringe camera when the device is measuring HD 98800 B. Consequently no special provisions are necessary in processing KI observations of HD 98800 B.

HST FGS Observations The HD 98800 system was observed by the Hubble Space Telescope Fine Guidance Sensors (FGS) in its “FGS-TRANS” mode and F583W filter on 20 epochs between 1996 and 2002. Of course, the FGS are also interferometers, but unlike the KI observations the FGS-TRANS data have been processed into estimated Ba-Bb separations by methods described in Franz et al. (1998). HD 98800 represents a challenging target for FGS observation: first because the B subsystem separation is near the resolution limit of the FGS, and second because (unlike the KI observations) the visual A component flux must be accounted for in data reduction. Because of these difficulties, of these 20 epochs only 11 of the measurements were deemed viable for triple-star analysis. These 11 B subsystem separation estimates are summarized in Table 3, which lists FGS separation data, model

Table 1. KI V^2 Calibration Objects Considered in our Analysis. The relevant parameters for our KI calibration object are summarized. Apparent diameter values are estimated from spectral energy distribution modeling based on archival photometry and spectral energy distribution templates from Pickles (1998).

Object Name	Spectral Type	V	K	HD 98800 Separation	Adopted Model Diameter (mas)
HD 97590	A6 V	7.3	6.7	2.6°	0.14 ± 0.04
HD 100219	F7 V	6.2	4.9	4.5°	0.44 ± 0.03

predictions, and data - model residuals relative to our “Joint-Fit” orbital solution (Table 4).

Orbital Solution In order to estimate the visual and physical orbit of HD 98800 B we have integrated the astrometric datasets described above with the double-lined radial velocity (RV) data on B presented in T95 Table 1. Figure 1 depicts our relative visual and spectroscopic orbit model of the HD 98800 B subsystem as derived in our “Joint-Fit” orbital solution (Table 4). The upper panel depicts the relative visual orbit model, with the primary (Ba) component rendered at the origin, and the secondary (Bb) component rendered at periastron. We have indicated the phase coverage of our KI V^2 data on the relative orbit with points (they are *not* separation vectors); the phase coverage of the V^2 data is sparse relative to other similar analyses (e.g. Boden et al. 2000). Because of this sparse phase coverage of the V^2 data, our initial visual orbit determination we constrained orbital parameters measured by RV (i.e. e , ω , P) to their T95 values (Table 4), and found an orbit model that phased-up acceptably with the T95 solution. Based on that constrained initial estimate, we then fully integrated the V^2 , FGS, and T95 RV data as described below (Table 4). The size of the HD 98800 B components are estimated (§ 3.1) and rendered to scale. The lower panel depicts the integrated double-lined spectroscopic orbit model and radial velocity data from T95.

Figure 2 depicts direct comparisons between our KI V^2 observations and predictions from our HD 98800 B “Joint-Fit” orbit model (Table 4; the five nights of data are each rendered in separate subpanels). The model is seen to be in good agreement with the KI data. Further, Figure 3 shows a direct comparison between the FGS separation data and the “Joint-Fit” visual orbit model. Again, the body of the FGS data are in good agreement with our orbit model, and the FGS phase coverage complements the phase coverage provided by the KI V^2 data.

In order to eliminate the possibility of multiple orbital solutions consistent with the relatively sparse KI data, we augmented our traditional Marquardt-Levenberg least-squares analysis (e.g. Boden et al. 2000) with a Bayesian parameter estimation analysis (Bretthorst 1988; Press et al 1992; Lay et al. 1997; Akeson et al 2002) using the integrated KI/FGS/RV dataset, an assumption of uniform priors in the orbital parameters, and a standard data likelihood function based on the chi-squared agreement between the observation set and orbit model:

$$P(D|Model) \propto \exp \left[- \sum_k \frac{(d_k - \hat{d}_k(Model))^2}{2\sigma_k^2} \right]$$

Figure 4 shows representative parameter estimate probability density distributions from this

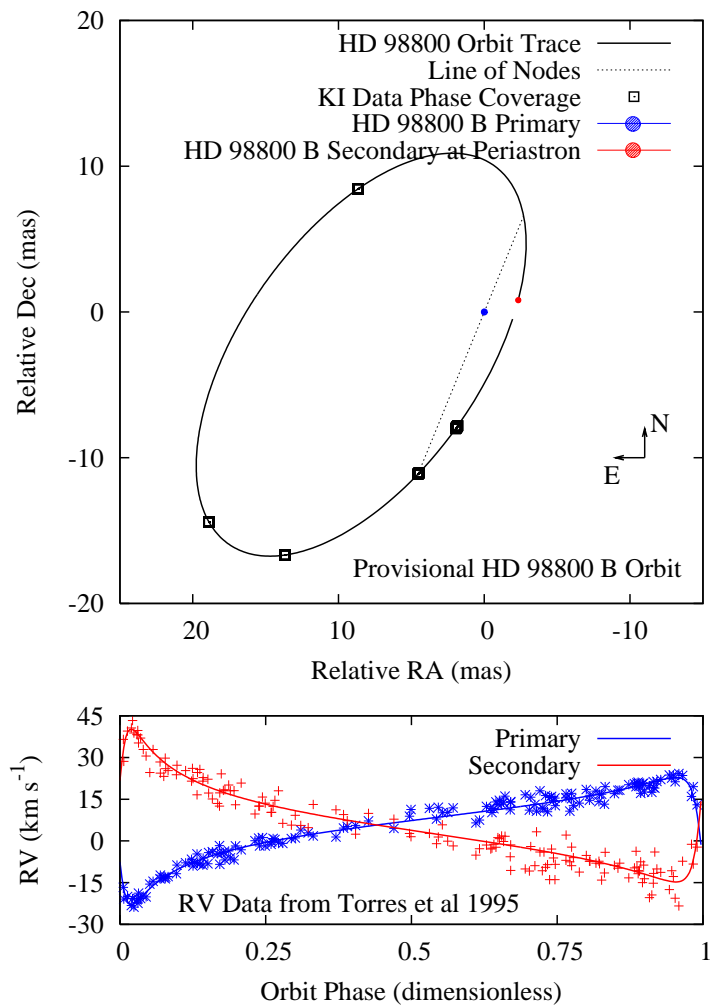


Fig. 1.— Orbit of HD 98800 B as derived in our “Joint-Fit” solution (Table 4). Upper Panel: the relative visual orbit model of HD 98800 B is shown, with the primary and secondary objects rendered at T_0 (periastron). The specific epochs where we have KI V^2 phase coverage are indicated on the relative orbit (they are not separation vector estimates). Component diameter values are estimated and rendered to scale. Lower Panel: the double-lined radial velocity orbit model and data from Torres et al. (1995).

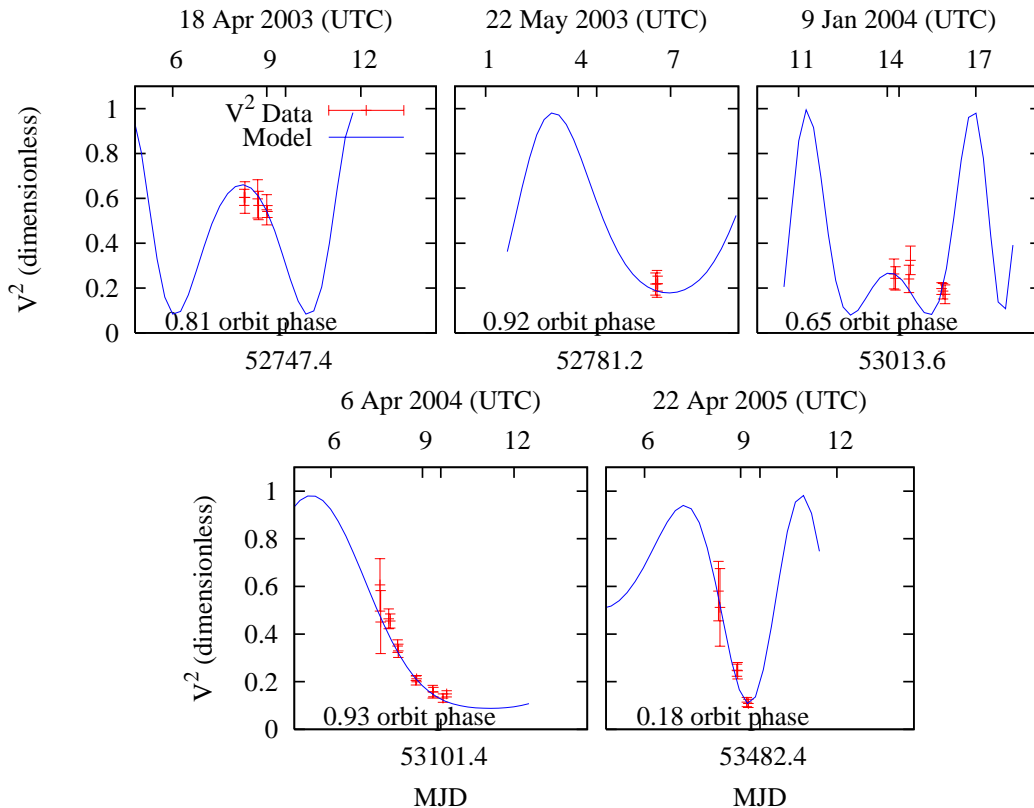


Fig. 2.— KI Data/Model Comparisons for HD 98800 B V^2 Observations. Here we give comparisons for our five epochs of KI V^2 observations (Table 2). In each case the data and model are shown.

process. The Bayesian analysis indicated no viable orbital solutions beyond the one presented here, and the orbital parameter estimates and uncertainties produced by the Marquardt-Levenberg and Bayesian analyses are in good agreement.

Orbital parameter estimates for the 98800 B subsystem are summarized in Table 4. Included for comparison are the double-lined orbital parameters on B from T95 (“T95”), the visual orbit parameters estimated holding P , e , and ω to their T95 values (“ V^2 Constrained”), and solutions integrating the KI V^2 and double-lined RV data from T95 (“ V^2 ”) and V^2 , FGS separations, and T95 RV (“Joint-Fit”). The various orbital solutions are in good agreement; the most notable variation ($\approx 2\sigma$) appears between the T95 and Joint-Fit period estimates based on the expanded time baseline of the combined dataset. In both the Marquardt-Levenberg and Bayesian orbital analysis we have weighted the astrometric datasets (KI and FGS) and T95 RV data equally and so as to yield a solution chi-squared per degree of freedom of 1: the resulting V^2 residual statistics are consistent with previous analyses from

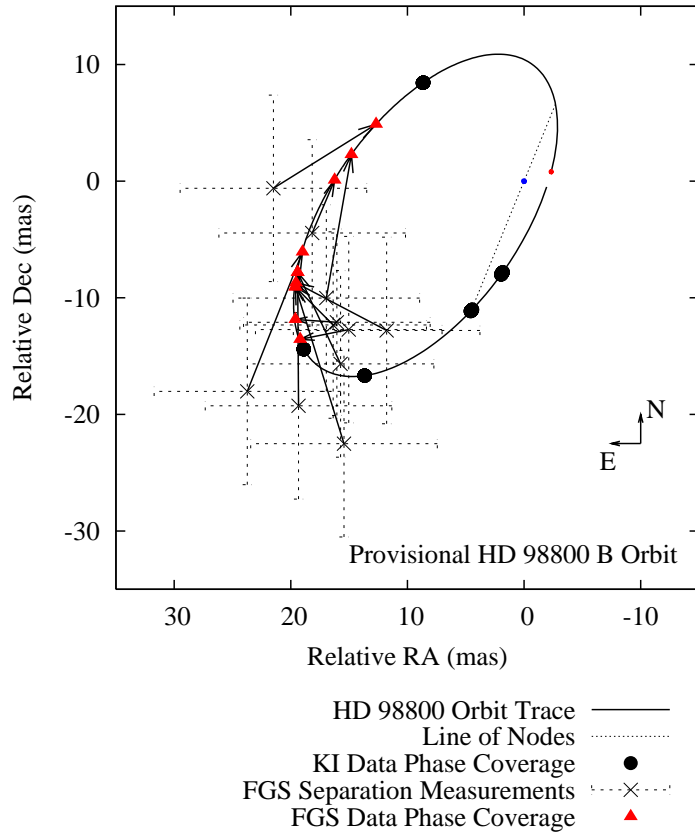


Fig. 3.— FGS Data/Visual Orbit Model Comparisons for HD 98800 B Observations. Here we give comparisons for our 11 epochs of reduced FGS observations (Table 3) and the “Joint-Fit” visual orbit model from Table 4. Arrows indicate the mapping of individual FGS separation estimates to corresponding points (phases) on the visual orbit model.

KI (Colavita et al 2003), and the FGS residual statistics are in reasonable agreement with previous FGS analyses given the complexity of the HD 98800 FGS data (e.g. Franz et al. 1998; Benedict et al. 2001). Uncertainties quoted in Tables 2 and 3 reflect the weightings in the Joint-Fit solution.

3. Physical properties of HD 98800 B

The orbital parameters from Table 4 allow us to directly compute many of the physical properties of the HD 98800 B subsystem and its components. Physical parameters derived from our HD 98800 B “Joint-Fit” integrated visual/spectroscopic orbit are summarized in Table 5. The limited V^2 phase coverage and resulting modest-precision orbital solution

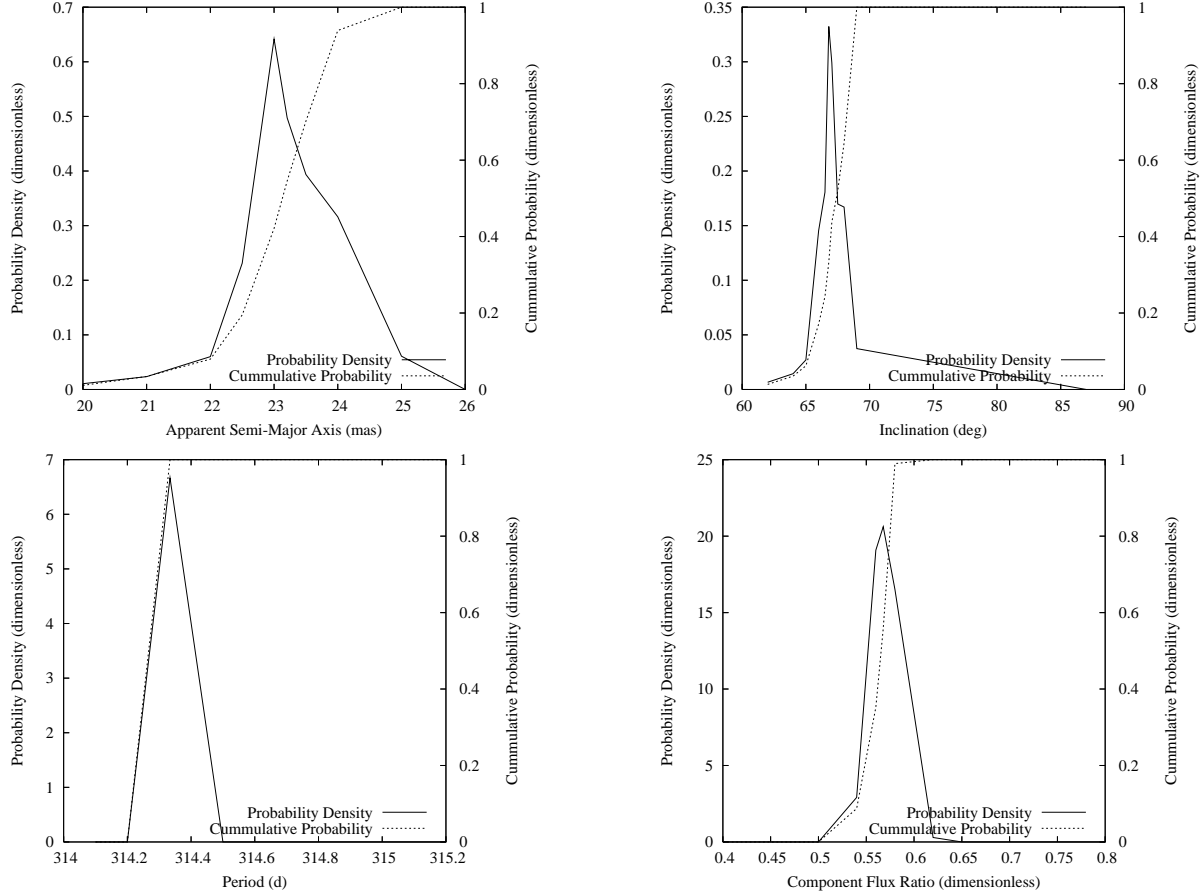


Fig. 4.— Bayesian Orbital Parameter Probability Density Estimates. To evaluate the uncertainties in our orbital model we conducted independent Marquardt-Levenberg least-squares and Bayesian parameter estimation analyses on the integrated KI V^2 /FGS/T95 RV dataset. Shown here are probability density and cumulative probability parameter estimates from the Bayesian analysis for four important orbital parameters (clockwise from top left: apparent semi-major axis (a), inclination (i), component intensity ratio, and period (P)). Agreement in orbital parameter values and uncertainties between the two independent analyses is good.

Table 4. Orbital Parameters for HD 98800 B. Summarized here are orbital parameters for the HD 98800 B system as determined by T95 and present results. We give three separate fits to our KI and FGS data: V^2 only (constrained in P , e , and ω to T95 values as indicated by brackets, “ V^2 Constrained”), KI V^2 integrated with T95 radial velocities (“ V^2 & RV”), and KI V^2 , FGS, and T95 RV (“Joint-Fit”). Note that the V-band Bb/Ba component flux ratio has been re-estimated based on the original T95 spectra; the revised value is given here.

Orbital Parameter	T95		This Work	
		V^2 Constrained	V^2 & RV	Joint-Fit
Period (d)	315.15 ± 0.39	[315.15]	314.334 ± 0.029	314.327 ± 0.028
T_0 (MJD)	48709.48 ± 0.30	52479.74 ± 0.38	52481.32 ± 0.23	52481.34 ± 0.22
e	0.7812 ± 0.0059	[0.7812]	0.7836 ± 0.0053	0.7849 ± 0.0053
K_{Ba} (km s $^{-1}$)	22.54 ± 0.37		22.87 ± 0.34	22.94 ± 0.34
K_{Bb} (km s $^{-1}$)	27.04 ± 0.62		27.45 ± 0.60	27.53 ± 0.61
γ (km s $^{-1}$)	5.73 ± 0.14		5.72 ± 0.14	5.73 ± 0.14
ω_{Ba} (deg)	109.5 ± 1.2	[109.5]	108.9 ± 1.1	109.6 ± 1.1
Ω (deg)		337.4 ± 3.2	337.8 ± 2.9	337.6 ± 2.4
i (deg)		66.7 ± 3.9	67.0 ± 3.7	66.8 ± 3.2
a (mas)		23.0 ± 3.5	23.2 ± 3.1	23.3 ± 2.5
ΔK (mag)		0.64 ± 0.18	0.616 ± 0.050	0.612 ± 0.046
ΔV (mag)	1.11 ± 0.15			

(Table 4) yields preliminary dynamical masses of 0.699 ± 0.064 and $0.582 \pm 0.051 M_{\odot}$ for the primary (Ba) and secondary (Bb) components respectively.

The Hipparcos catalog lists the parallax of HD 98800 as 21.43 ± 2.86 mas, corresponding to a system distance of 46.7 ± 6.2 pc (ESA 1997). The distance determination to HD 98800 B based on our orbital solution is 42.2 ± 4.7 pc, corresponding to an orbital parallax of 23.7 ± 2.6 mas, consistent with the Hipparcos result at 9.5% and 0.6-sigma.

At the distance of HD 98800 neither of the B subsystem components are significantly resolved by the KI K-band fringe spacing, and we must resort to model diameters for the components. We have estimated the HD 98800 B component apparent diameters through spectral energy distribution modeling. We find apparent diameters of 0.238 ± 0.017 and 0.188 ± 0.014 mas for the Ba and Bb components respectively (details of the spectral energy distribution modeling are given in §3.1). With our system distance estimate these estimated diameters correspond to physical radii of 1.09 ± 0.14 and $0.85 \pm 0.11 R_{\odot}$, and (combined with the mass estimates) log surface gravities of 4.21 ± 0.12 and 4.34 ± 0.12 for the Ba and Bb components respectively.

3.1. Spectral Energy Distribution Modeling

Because interferometric observations potentially resolve the stellar components in a binary system, we always construct spectral energy distribution (SED) models for binary systems to estimate a priori apparent diameters. For HD 98800 B SED modeling results are particularly interesting in light of a conjecture by Tokovinin (1999) that the putative B circumbinary disk (P2001) obscures our view [of the B sub]system to explain the irregular low-level photometric variability observed by Hipparcos (S98).

P2001 summarizes the body of A/B-resolved flux measurements in the HD 98800 system, and has modeled SEDs of the A and B subsystems with Kurucz templates. To the P2001 flux data we add Bb/Ba flux ratio estimates based on our visibility and spectroscopic observations. We estimate a Bb/Ba flux ratio of 0.36 ± 0.05 at 519 nm in the CfA spectroscopy based on the original spectra. This estimate is different than the original T95 value – it includes a correction related to the different normalization of the template spectra used in T95, which was overlooked in the original analysis. At $2.2 \mu\text{m}$ the flux ratio is 0.569 ± 0.024 from the KI visibility data (Table 4). Using a custom two-component SED modeling code, we have modeled the B subsystem flux and ratios using solar and sub-solar abundance SED templates from Kurucz (2001), Lejeune et al (1997, 1998), and Pickles (1998), and compared the flux and ratio data with a large grid of SED templates for each component

Table 5. Physical Parameters for HD 98800 B. Summarized here are the physical parameters for the HD 98800 B subsystem as derived from the “Joint-Fit” solution orbital parameters in Table 4, and SED modeling.

Physical Parameter	Ba Component	Bb Component
a (10^{-1} AU)	4.47 ± 0.13	5.36 ± 0.13
Mass (M_{\odot})	0.699 ± 0.064	0.582 ± 0.051
System Distance (pc)	42.2 ± 4.7	
π_{orb} (mas)	23.7 ± 2.6	
T_{eff} (K)	4200 ± 150	4000 ± 150
Model Diameter (mas)	0.239 ± 0.017	0.188 ± 0.014
Bolometric Flux (10^{-9} erg cm $^{-2}$ s $^{-1}$)	5.96 ± 0.28	3.00 ± 0.15
Luminosity (L_{\odot})	0.330 ± 0.075	0.167 ± 0.038
Radius (R_{\odot})	1.09 ± 0.14	0.85 ± 0.11
log g	4.21 ± 0.12	4.34 ± 0.12
M_K (mag)	3.80 ± 0.25	4.38 ± 0.25
M_V (mag)	6.91 ± 0.26	8.02 ± 0.27
$V-K$ (mag)	3.11 ± 0.12	3.61 ± 0.14

ranging in temperature (spectral type) from 3500 – 5000 K (M3 – K2). Good fits were found with both Lejeune and Pickles SED templates, and the results consistently preferred temperature of 4200 ± 150 K for Ba and 4000 ± 150 K for Bb; these values are consistent with results from other studies (e.g. S98, P2001). Figure 5 depicts the best-fit results from Lejeune template comparisons. Component temperatures, angular diameters, and related quantities in Table 5 are composite values from Lejeune and Pickles SED model results.

Notable in the SED solutions is the necessity to include a small amount of extinction ($A_V \sim 0.3 \pm 0.05$) to model the observed B subsystem flux distribution. S98 reached a similar conclusion in their analysis of Li-line spectral observations (including this finding as part of their favored hypothesis for the B component parameters). It is tempting to take this extinction as corroboration of Tokovinin’s conjecture that B circumbinary material lies along the line of sight to the stellar components. As a cross-check of this hypothesis we ran a similar series of SED models for the A component (the Ab component was taken to contribute zero flux), and found that no extinction was necessary to fit the A flux distribution. Based on our SED modeling it appears that there is a source of extinction along our line of sight to B that is absent to A.

P2001 has argued that the putative B circumbinary disk is likely coplanar with the B orbital plane. A simple coplanar disk would require an aspect ratio or flaring of at least $\tan(90 - 67) \approx 0.42$ for such a disk to be the source of this extinction. Alternatively, it seems likely that a B circumbinary disk would be disrupted by the A – B orbit, so the presumption of simple disk co-planarity with the B orbit may not be well founded. It seems direct resolution and mapping of the B circumbinary disk will be critical to understand the B circumbinary material distribution in the highly dynamic HD 98800 system.

4. Discussion

4.1. Comparison with stellar evolution models

Hillenbrand & White (2004) have shown that PMS models are in good agreement with dynamically determined masses above $1.2 M_{\odot}$. However, below $1.2 M_{\odot}$ the existing models do a poorer job of matching observed component properties, tending to predict hotter and more luminous stars for a given mass. Of course, it is exactly this kind of apparent model/observation discrepancy that makes HD 98800 such a compelling system for careful study. While the orbit results presented here are preliminary, it is still interesting to make some initial comparisons between our observations and PMS evolutionary models.

Our inferred radiometric parameters for the HD 98800 B components (Table 5) are in

good agreement to those found in previous work (S98, P2001), so comparisons with PMS models largely go along similar lines. Figure 6 shows the position of the B subsystem components in luminosity/ T_{eff} space, along with PMS evolutionary models from Siess et al (2000) and Baraffe et al. (1998). Model evolutionary tracks for masses that bracket the component masses inferred from our orbit model are emphasized in the figure. As found by P2001, for solar metallicity (Figure 6 left panels) the radiative properties of the Ba and Bb components predict component masses that are significantly higher than our orbit model would indicate. This naturally led P2001 to infer a B orbital inclination ($\sim 58^\circ$) that is similar but slightly lower than the orbit model presented here. Both Siess et al (2000) and Baraffe et al. (1998) models predict slightly cooler and less luminous components at the low masses indicated by our orbit model.

The apparent model/observation discrepancy is reduced if we consider the possibility that elemental abundances for HD 98800 components are sub-solar. S98 attempted an abundance estimate for HD 98800, and argue for solar abundance with an uncertainty of ~ 0.2 dex. Figure 6 right panel shows the same comparison of component properties with Siess et al (2000) models at $[M/H] = -0.3$ (allowed by S98), and Baraffe et al. (1998) models at $[M/H] = -0.5$ (probably not allowed by S98). The match between the lower abundance models at our inferred component masses and radiometric properties is improved, with both components matching the relevant mass tracks within the temperature error bars for both the lower abundance Siess et al (2000) and Baraffe et al. (1998) models. From superimposed isochrones in Figure 6 we infer the HD 98800 age is in the 8 – 20 MYr range, consistent with previous findings (S98).

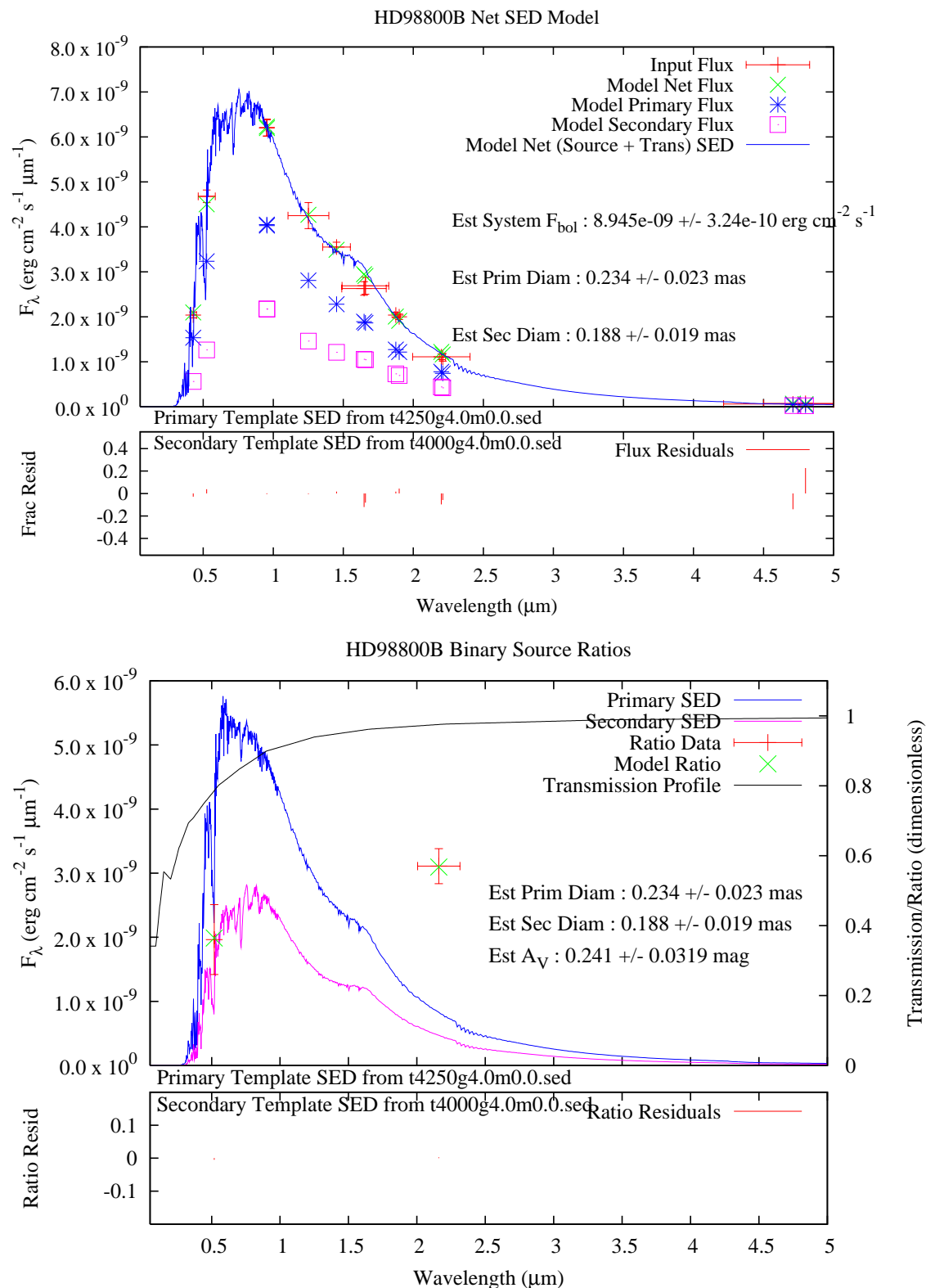


Fig. 5.— Sample Spectral Energy Distribution Model for HD 98800 B. Here SED templates from Lejeune et al (1997, 1998) have been used to simultaneously model published flux measurements (summarized in P2001 Table 2; top) and component flux ratio estimates (Table 4; bottom) from our KI V² and T95 spectroscopic measurements.

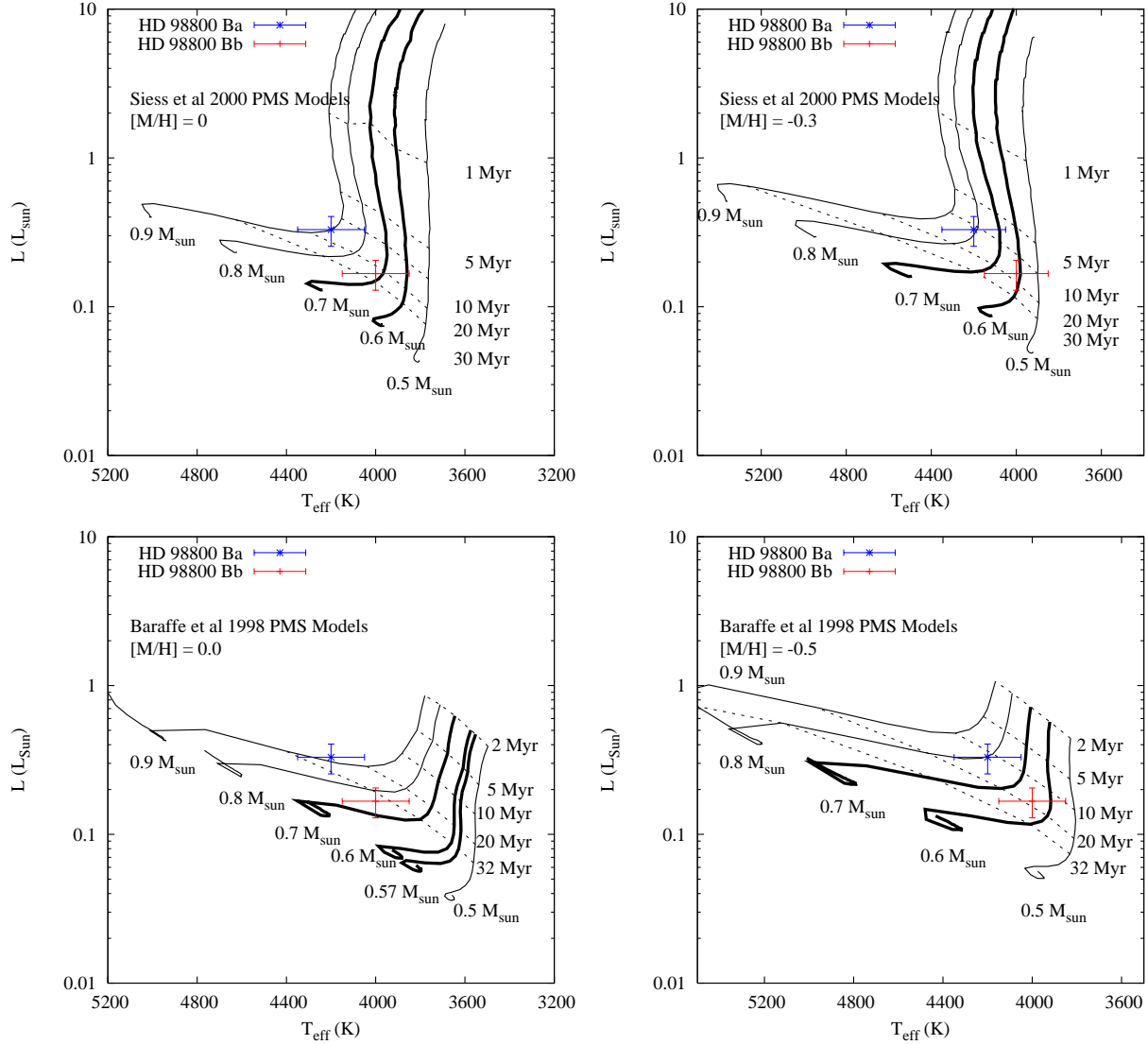


Fig. 6.— HD 98800 B Components Compared With PMS Models. Here we show the HD 98800 B components in luminosity/ T_{eff} space, and PMS evolutionary tracks by Siess et al (2000) (top panels) and Baraffe et al. (1998) (bottom panels). As found by P2001, solar abundance models (left panels) suggest higher masses for the HD 98800 B than our orbit yields, however a lower abundance ($[M/H] = -0.3 - -0.5$, right panels) for the components brings the inferred masses and radiative properties into better agreement with model predictions from both families. On all panels bold lines emphasize mass tracks bracketing component mass values implied by the orbit model (Table 5), and isochrones at spanning a range of ages between 1 and 32 Myrs are given.

4.2. Conclusions and Future Work

The preliminary orbit presented here for HD 98800 B does an excellent job of matching up with other empirical constraints on the system: it independently phases properly with the T95 RV solution, and it yields a distance estimate that agrees well with the Hipparcos determination. The inclination of the orbit model raises interesting questions concerning the nature of the putative B circumbinary disk. A planar disk and strict orbit/disk co-planarity would imply a thick aspect ratio or flaring for the disk (≈ 0.4) if it produces the inferred extinction along the line of sight to the B components, however perturbations to the disk from the outer A-B orbit seem likely. Further, the implied physical semi-major axis of the B orbit (Table 5; 0.98 ± 0.02 AU) fits within previous estimates of the inner disk radius of 1.5 – 2 AU (S98, P2001), but it is unclear whether the implied separation is consistent with dynamical modeling of such circumbinary disks (e.g. Artymowicz & Lubow 1994; Pichardo et al 2005).

The orbit model presented here implies component dynamical masses accurate to approximately 8%; with such mass determinations we can not yet provide critical tests for low-mass PMS stellar models. *Prima facie* comparisons with PMS models from Baraffe et al. (1998) and Siess et al (2000) suggest that the components are hotter and more luminous than predicted by the models for solar abundance, and considering the possibility of slightly sub-solar abundance brings the inferred component parameters into better agreement with the model predictions. However at present the significant dynamical mass and effective temperature errors do not yet allow for definitive conclusions. Narrowly it is important to establish the abundance of HD 98800 to properly test and refine PMS models. More broadly it is intriguing to consider the possibility that stars as young as TWA members may have significantly sub-solar abundances.

The B subsystem orbit presented here is preliminary, and we are continuing observation of the system interferometrically and spectroscopically to refine the orbit model, and resulting component properties and system distance. The apparent inclination for B is such that additional observations are likely to result in significantly refined component parameter estimates. A forthcoming publication will provide a more detailed comparison between the B component parameters and PMS models based on a refined B subsystem orbit model. Further, we have also observed HD 98800 A with KI on two epochs, and the V^2 data show clear signs of resolving that subsystem as well – the first time the Ab component has been directly detected. We will continue to observe A to determine its orbit and component properties as well.

The authors wish to thank the anonymous reviewer for the many thoughtful comments

that have greatly improved this manuscript.

Part of this work was performed at the Michelson Science Center (MSC), California Institute of Technology under contract with the National Aeronautics and Space Administration (NASA).

Some of the data presented herein were obtained at the W.M. Keck Observatory, which is operated as a scientific partnership among the California Institute of Technology, the University of California and the NASA. The Observatory was made possible by the generous financial support of the W.M. Keck Foundation. We gratefully acknowledge the support of personnel at the Jet Propulsion Laboratory, W.M. Keck Observatory, and the MSC in obtaining KI observations of HD 98800. The authors wish to recognize and acknowledge the very significant cultural role and reverence that the summit of Mauna Kea has always had within the indigenous Hawaiian community. We are most fortunate to have the opportunity to conduct observations from this mountain.

GT acknowledges partial support from NASA’s MASSIF SIM Key Project (BLF57-04) and NSF grant AST-0406183.

This research has made use of services of the MSC at the California Institute of Technology; the SIMBAD database, operated at CDS, Strasbourg, France; of NASA’s Astrophysics Data System Abstract Service; and of data products from the Two Micron All Sky Survey, which is a joint project of the University of Massachusetts and the Infrared Processing and Analysis Center, funded by NASA and the National Science Foundation.

REFERENCES

- Akeson, R., Ciardi, D., van Belle, G., and Creech-Eakman, M. 2002, *ApJ* 566, 1124.
- Andersen, J. 1991, *A&A Rev.* 3, 91
- Artymowicz, P. and Lubow, S. 1994 *ApJ* 421, 651.
- Baraffe, I., Chabrier, G., Allard, F., and Hauschildt, P. 1998, *A&A* 337, 403.
- Benedict, G. et al. 2001, *AJ* 121, 1613.
- Boden, A., Creech-Eakman, M., and Queloz, D. 2000, *ApJ* 536, 880.
- Bretthorst, G. 1988, *Bayesian Spectrum Analysis and Parameter Estimation* (New York: Springer)
- Colavita, M. et al 2003, *ApJ* 592, L83.
- ESA 1997, *The Hipparcos and Tycho Catalogues*, ESA SP-1200.
- Franz, O., et al. 1998, *AJ* 116, 1432.
- Hillenbrand, L. & White, R. 2004, *ApJ* 604, 741.
- Hummel, C. et al. 2001, *AJ* 121, 1623.
- Innes, R. 1909, *Transvaal Obs. Circ* 1, 1.
- Koerner, D. et al 2000, *ApJ* 533, L37.
- Kurucz, R. 2001, Kurucz models used here are available at <http://cfaku5.cfa.harvard.edu>.
- Lay, O., Carlstrom, J., and Hills, R. 1997, *ApJ* 489, 917.
- Lejeune, T. et al 1997, *A&AS* 125, 229.
- Lejeune, T. et al 1998, *A&AS* 130, 65.
- Palla, F. & Stahler, S. 2001, *ApJ* 553, 299.
- Pichardo, B. et al 2005, *MNRAS* 359, 521P (astro-ph/0501244).
- Pickles, A. 1998, *PASP* 110, 863.
- Prato, L. et al 2001, *ApJ* 549, 590 (P2001).

- Press, W. et al 1992, Numerical Recipes (New York:Cambridge University Press)
- Siess L., Dufour E., & Forestini M. 2000, A&A 358, 593.
- Simon, M, Dutrey, A. & Guilloteau, S. 2000, ApJ 545, 1034.
- Soderblom, D. et al 1996, ApJ 460, 984.
- Soderblom, D. et al 1998, ApJ 498, 385 (S98).
- Steffen, A. et al 2001, AJ 122, 997.
- Tokovinin, A. 1999, Ast. Lett. 25, 669.
- Torres, G. et al. 1995, ApJ 452, 870 (T95).
- Walker, H. & Walstencroft, R. 1988, PASP 100, 1509.
- Webb, R. et al 1999, ApJ 512, L63.
- Zuckerman, B. & Becklin, E. 1993, ApJ 406, L25.